Journal of Magnetism and Magnetic Materials 531 (2021) 167984

Contents lists available at ScienceDirect

Journal of Magnetism and Magnetic Materials

journal homepage: www.elsevier.com/locate/jmmm

First-principles calculation of magnetic, structural, dynamic, electronic, elastic, thermodynamic and thermoelectric properties of Co_2ZrZ (Z = Al, Si) Heusler alloys

S. Sâad Essaoud [a,b,*], Ahmed S. Jbara [c,d]

[a] Department of Physics, Faculty of Science, University of M'sila, 28000 M'sila, Algeria
[b] Laboratoire de Physique des Particules et Physique Statistique, Ecole Normale Supérieure-Kouba, BP 92, Vieux-Kouba, 16050 Algiers, Algeria
[c] Mathematics Department, College of Education for Pure Science, Al-Muthanna University, Samawah 66001, Iraq
[d] Physics Department, Science College, Al-Muthanna University, Samawah 66001, Iraq

ARTICLE INFO

Keywords:
Heusler Alloys
Half-metallic
Seebeck Coefficient
Electrical and thermal conductivity coefficients
Elastic Constants

ABSTRACT

Electronic, magnetic, dynamic, elastic, thermodynamic, and thermoelectric properties for Co_2-based full Heusler alloys are investigated theoretically. The full potential–linearized augmented plane wave (FP-LAPW) method within density functional theory (DFT) incorporated on WIEN2k code is employed in our calculation. Through this study, we found that the FM-$L2_1$ is the most magnetic-structure stable phase for both Co_2ZrAl and Co_2ZrSi compounds, as well as they, are dynamically stable where all the calculated of the optic and acoustic phonon frequencies have positive values. Band structure calculation demonstrated that all compounds exhibit band gaps of about 0.88 and 1.54 eV using mBJ-GGA potentials for Co_2ZrAl and Co_2ZrSi in a localized minority spin channel (unlike the other direction which appears a metallic behavior) with high spin polarization (100%) in its ground state. Under high pressure, both compounds keep the same electronic behavior in both spins' channels with a little decreasing in gap energy, unlike the total magnetic moment which doesn't change. The semi-local Boltzmann transport theory has been used to investigate thermoelectric properties and we found that both compounds exhibit a high Seebeck coefficient and high-power factor up to 1.25 mV/K for Co_2ZrSi. Also, the quasi-harmonic model has been applied to study the temperature effect on heat capacities at constant volume, in which entropy, Debye temperature and lattice thermal conductivity are analyzed and discussed. To get more information about the elastic behavior; the elastic stability in the equilibrium state and under two pressures values (12 GPa and 24 GPa) are found. The findings predicted the stability of these compounds' properties with and without pressure, which makes them candidate materials for devices fabrication in several areas such as spinotronic, thermoelectric, shape-memory and spin filters.

1. Introduction

In recent years, the industrial field has become in need to find environmentally friendly alternative energy sources, where many attempts to produce electrical energy by obtaining it depending on another source. Conversion of the thermal energy into electricity (thermoelectric application) is one of the most important technologies, especially those that depend on the Seebeck effect which has received great attention because this technology allows us to recover unused thermal energy (the thermal energy that emitted out by motors and electronic devices), also, The most important feature of thermo-electric converters is that they depend on the properties of the solid material and do not need moving elements, liquid materials or harmful gases. The electrical energy produced in thermo-electric transducers under the influence of Seebeck depends on temperature differences, of course, but also on the properties of the materials used such as conductors and semiconductors the study carried out in 2017 by Abdel-Motaleb and Qadri [1] seems that metals exhibit low Seebeck coefficients, unlike semiconductors, which exhibit somewhat larger Seebeck coefficients.

Heusler alloys are Among many materials that have a semiconductor behavior where half and full Heusler alloys have given great motivation to the development of new technologies devices from the first moment of their discovery by Friedrich Heusler in 1903[2]. Due to their rich properties, these materials can behave as metallic, semiconductors,

* Corresponding author at: Department of Physics, Faculty of Science, University of M'sila, 28000 M'sila, Algeria.
E-mail addresses: saber.saadessaoud@univ-msila.dz (S. Sâad Essaoud), ahmedsbhe@mu.edu.iq (A.S. Jbara).

https://doi.org/10.1016/j.jmmm.2021.167984
Received 13 November 2020; Received in revised form 27 March 2021; Accepted 27 March 2021
Available online 2 April 2021

semimetals in different types of magnetic order such as ferromagnets, antiferromagnets and half-metallic ferromagnets. These materials have attracted much attention especially in the manufacture of power generation devices, solid-state refrigerators and thermoelectric devices [3,4], which allows to convert waste heat into useful electricity and reduce the energy consumption which is lost as heat form. The wide use of thermoelectric devices in daily life has encountered by several problems, the most important that the materials used are in low abundance and require careful accurate doping and complex synthesis processes, which raises their industry cost. The optimum choice of efficient thermoelectric materials is the core of much theoretical and experimental research where the efficient performance of thermoelectric material is evaluated through the dimensionless figure of merit (ZT) ($ZT = \frac{S^2\sigma T}{\kappa}$ where S is the Seebeck coefficient, σ is the electrical conductivity, κ is the total thermal conductivity, and T is the absolute temperature), so we can obtain high performance of the thermoelectricity when the thermoelectric material has high electrical conductivity, high Seebeck coefficient and low thermal conductivity values. Finding a metal that achieves these three conditions is very difficult because these factors are not independent of each other and cannot be controlled individually. For example, raising electric conductivity often leads to the decreasing of the Seebeck coefficient or raising the thermal conductivity. Bi_2Te_3 and Sb_2Te_3 [5,6] and its alloys are among the most important materials that gave good theoretical and experimental results at room temperature, mechanical, magnetic and electronic stability under pressure effect of these compounds, production cost (tellurium is an expensive element) and the toxicity of the tellurium element made them undesirable materials, especially at very high temperatures [7,8].

With the great importance of thermal-electric technology particularly by alternative energies, it has become a great challenge to found new materials which are cheap, environment-friendly, easy to synthesize. Many of these new materials are not suitable for large-scale application because of complex and expensive or contained a toxic element. An analysis of some theoretical and experimental studies of electronic band structure considered the half-Heusler alloys which behave as semiconductors (narrowband gaps) are efficient thermoelectric materials [9,10]. Tino Jaeger et al [11] reported that Half-Heusler alloys like MNiSn (M = Ti, Zr, and Hf) are promising candidates to increase the thermoelectric figure of merit ZT by decreasing thermal conductivity. Mastronardi et al [12] in his studies shows that the half-Heusler alloys based on LnPdSb, where Ln = Ho, Er, and Dy are successful thermoelectric (TE) materials and maybe a general characteristic of the large class of semiconducting materials with the half-Heusler structure type, and that related compounds yet to be tested may also be excellent thermoelectric.

Recently the new research interest has been focused on the new full Heusler (FH) alloys due to its mechanical properties, stability, high Curie temperature, and their environment-friendly constituents. Some theoretical studies revealed that several Heusler alloys have ZT values are around unity one [13]. Teng Fang et al [14] found that Half-Heusler (HH) compounds, with a valence electron count of 8 or 18, have gained popularity as promising high-temperature thermoelectric (TE) materials due to their excellent electrical properties, robust mechanical capabilities, and good high-temperature thermal stability.

Ternary Heusler alloys have X_2YZ formula composed by three elements: X and Y are two transition metals while the Z is in the p-block and in some cases. Recently, compounds with Mn_2 and Co_2 based are among the most studied families, Mn_2-based Heusler alloys have been studied both experimentally and theoretically where the half-metallicity behavior of compounds was explored [15–19]. Cobalt full Heusler alloys family have studied by Shakeel et al [20] for both Co_2ScSb and Co_2TiSb compounds under High Pressure-Temperature effects and the half-metallic behavior has been confirmed with an indirect energy gap. Other compounds with Co_2 based Heusler are studied in different ways like $Co_2Cr_{1-x}Mn_xAl$ [21] , Co_2YZ (Z = P, As, Sb, and Bi) [22], Co_2YAl (Y = Fe, Ti) [23] and X_2YZ (X = Co, Y = Mn, Z = Si/Ge) [24].

Our work is mainly based on the Co_2ZrAl and Co_2ZrSi compounds as Co_2 based Heusler compounds, where we aim behind this work primarily to verify the stability of the characteristic properties of these type of compounds, such as the half-metallic electronic behavior, the total magnetic moment value, as well as their elastic properties, and to check-up whether these characteristics would change under the influence of any pressure affecting them. Therefore, we have examined the stability of the two compounds, in terms of structural, electronic, magnetic, and mechanical (elastic) properties. This work is achieved by calculating several coefficients and parameters of the aforementioned properties at certain pressures. Also, we explored the thermodynamic and thermoelectric properties under the temperature influence.

2. Computational details

Our calculations were carried out using the FP-LAPW method, as implemented in the WIEN2k code [25]. The exchange–correlation interaction was treated using the generalized gradient approximation (GGA) by Perdew, Burke, and Ernzerhof (PBE) potential [26] in all studied properties. On the other hand, the modified Becke-Johnson potential (mBJ) [27] was adopted to obtain the electronic band structure, total (DOS), and partial (PDOS) densities. Getting accurate results requires a well-chosen of the entered parameters, so we divided the unit cell into two regions; inside the no overlapping atoms sphere, in this case, the charge density and the potential are expressed via spherical harmonic expansion, so, we had chosen 2.1, 2.2 atomic units (a.u) as R_{MT} radius of Co, Zr and 2.0 for Al and Si atoms. While outside the atomic spheres, the wave functions are expanded in terms of plane waves with a wavevector cutoffs of $R_{MT} * K_{max}$ equal to 9 for all compounds where K_{max} is the largest reciprocal lattice vector used in the plane wave expansion and R_{MT} represents the smallest MT sphere radii. For Brillouin zone (BZ) integration, 72 special k-points for all alloys in the irreducible wedge have been used to minimize the total energy for all compounds. Checking the dynamic stability was done through phonon band dispersion and phonon DOS analysis of both compounds using the PHONOPY package [28].

To study the elastic properties of the cubic structure to which Co_2ZrAl and Co_2ZrSi compounds belong, it is necessary to calculate three independent elastic constants C_{11}, C_{12} and C_{44}. This is done by applying small strains to the unstrained lattice and then using Taylor expansion of the total energy of the system.

The electronic configurations (for valence electrons) are for Co: $3d^74s^2$, Zr: $4d^2\ 5\ s^2$, Al: $3s^23p^1$ and Si: $3s^23p^2$. The separation energy between valence and core states was set to − 6 Ry. The charge convergence was set to 10^{-3} and simultaneously the energy convergence criterion was set to 10^{-5}. Also, the electronic properties are calculated within the modified Becke Johnson approximation (mBJ) [27] which serves for optimization of the corresponding potential for electronic band structure calculations. To calculate the thermoelectric transport properties, we have used BoltzTraP code [29], which is based on semi-classical Boltzmann theory. Effect temperature and pressure on thermodynamic properties such as heat capacity, Debye temperature entropy .etc. are estimated using the quasi-harmonic approximation implemented GIBBS2 code [30,31].

X_2YZ Heusler alloys contain four atoms, according to the position occupied by these atoms, we distinguish two types of structures symbolized $L2_1$-type (Cu_2MnAl structure, space group Fm-3 m (225)) and X_α (Hg_2CuTi type) with space group F-43 m (216). Each atom in the alloys can occupy one of the following four sites: A(0.0.0), B(1/4.1/4.1/4), C (1/2.1/2.1/2), and D (3/4.3/4.3/4). As it is also known that the physical properties of crystals depend directly on their structural properties, therefore any change in the arrangement of the atoms' position in all the two phases affects the properties of the compound as we will see later. In both types of structures, X and Z atoms take places A and D, while the difference between the two phases remains in the place that the atom Y

will occupy. As shown in Fig. 1, we note that the Y atom takes place C in the X_α phase, while it occupied B site in the other phase ($L2_1$).

3. Results and discussions

3.1. Structural-magnetic and dynamic stability of Co_2ZrZ(Z = Al, Si) Heusler alloys

In order to estimate the lattice constants, bulk modulus and the cohesive energy of Co_2ZrZ (Z = Al, Si) corresponding to the ground state structure of each alloy; and to find the favorable magnetic state, we compute the total energy E of the cell at different volumes V for the two different possibilities of site occupations in three different magnetic orders (ferromagnetic (FM), paramagnetic (PM) and anti-ferromagnetic (AFM)) and fitting the obtained data with Murnaghan equation Eq. (1) of state (EOS)[32] given by the formula:

$$E(V) = E_0 + \frac{B}{B'(B'-1)}\left[V\left(\frac{V_0}{V}\right)^{B'} - V_0\right] + \frac{B}{B'}(V - V_0) \quad (1)$$

where E_0 and V_0 are the total energy and the volume at equilibrium, respectively. B and B' are the modulus of compressibility and its derivative, respectively.

Fig. 2 shows the total energy-volume curves of $L2_1$ and X_α-type structures for Co_2ZrAl and Co_2ZrSi compounds in FM, PM and AFM states. our results exhibit that both compounds in $L2_1$ type with ferromagnetic arrangement have the lowest energies at the equilibrium state, thus, they are energetically more stable compared to paramagnetic and antiferromagnetic in $L2_1$ type and X_α-type whatever its magnetic states where the difference in the total energy between the $L2_1$-type (FM) structure and X_α-type (FM) structure is too large for both compounds and it reached to 0.12 Ry and 0.11 Ry for Co_2ZrAl and Co_2ZrSi compounds respectively. The lattice parameter, bulk modulus and cohesive energy for all compounds in all type structures are calculated using GGA approximation and compared to other studies on Table 1 in both ferromagnetic, antiferromagnetic and paramagnetic states, in our work the obtained results for lattice parameters in FM state confirm what was achieved in the other study that he conducted by Ghosh et al [33]. Bulk modulus symbolized B is a measure of the substance's resistance to uniform compression and its obtained values is presented in Table1. Indeed, both compounds have a high value of bulk modulus 165.79–182.52 GPa for Co_2ZrAl and Co_2ZrSi in $L2_1$ type with FM state respectively confirm the high hardness of the considered compounds.

Coherent of compounds and physical stability of the Co_2ZrAl and Co_2ZrSi can be studied via the cohesive energy, this latter expresses the energy needed to separate a solid into its various free constituents. In ab-initio calculations, the cohesive energy of the Co_2ZrZ alloys is the difference between the calculated total energy at the equilibrium point of an elementary cell and the energy of its isolated atoms Co, Zr and Z like the formula Eq. (2):

$$E_{coh} = \frac{(2E^{Co}_{atom} + E^{Zr}_{atom} + E^{Z}_{atom}) - E^{Co_2ZrZ}_{tot}}{N_{Co} + N_{Zr} + N_Z} \quad (2)$$

where N_{Co}, N_{Zr}, and N_Z are the number of Co, Zr, and Z atoms in the unit-cell of Co_2ZrZ compound. According to the calculated results, we can see that both compounds have high cohesive energy in $L2_1$-type where Co_2ZrSi (6.13 eV) is more coherent than Co_2ZrAl (5.84 eV) compound these interesting marks emphasize the stability of these compounds. The calculated total and partial magnetic moments per formula unit codified in Table.1 are integer for all Heusler alloys studied in this work in FM state and equal to $1\mu_B$ for Co_2ZrAl and $2\mu_B$ Co_2ZrSi. The main contribution to the magnetic moment in the total magnetic moment is due to Cobalt atoms in A and C sites and they have equal magnetic moments in parallel order whereas in the case of antiferromagnetic state, Cobalt atoms had antiparallel magnetic moments where the total magnetic moment is zero. Our results are in good agreement with the previous results [33] and verified the Pauling-Slater rule [34,35], which is easily expressed in the following relation $M_{tot} = (N_{ve}\text{-}24)\ \mu_B$, where M_{tot} is the total magnetic moment and N_{ve} is the number of valence electrons (N_{ve} (Co_2ZrAl) = 25 and N_{ve} (Co_2ZrSi) = 26).

Now, we want to study the magnetic stability of both compounds under the influence of pressure which leads to compression or dilatation of the unit cell and thus an increase or decrease in the lattice constant. In Fig. 2, we plot the changes in both the total and partial magnetic moments of the atoms in terms of the lattice constant. Also, it is evident that the total magnetic moment (horizontal straight line) remains constant despite the change of the lattice constant. Also, both cobalt atoms in A and C sites have an equal magnetic moment which increases with increasing the lattice constant, unlike Aluminum, Zirconium, Silicon atoms and the interstitial zone where the magnetic moment values decrease with increasing the lattice constant. The obtained results proved the magnetic stability of the two studied compounds under the influence of pressure.

The determination of the most magnetic-structural stable phase using WIEN2k code was performed at zero temperature, which is based on the Born-Oppenheimer approximation [36] to neglect the effect of temperature that causes the atom's vibration around their equilibrium position. In this part, we want to study the dynamic stability of the Co_2ZrAl and Co_2ZrSi compounds, where we will be able to calculate the vibration frequencies as well as know the response of the crystal lattice to any distortion resulting from atoms displacement around their equilibrium position. To the best of our knowledge, the vibration of the N atoms forming the primitive cell of the compound creates 3 N number of phonon branches, 3 of which are acoustic and the remaining (3 N-N) as optic branches, in our work both Co_2ZrAl and Co_2ZrSi consist of 4 atoms, thus, we will found 12 total branches (3 acoustic and 9 optical branches).

To evaluate both phonon band dispersion, total and projected phonon density DOS, we have generated 2 × 2x 2 supercell, so we will get two primitive cells along each of the three directions (x, y and z). We calculated its phonon dispersion in the first Brillouin zone along the high symmetric path (W /L/ Γ/ X /W /K). Fig. 3 shows phonon dispersion spectra, the total and projected phonon density of states of Co2ZrZ (Z = Al, Si) at 0 GPa pressure. Band phonon spectra analysis appears that both compounds have an almost similar shape without any gap separating acoustic than optical modes, and we can see that all phonon branches (whether acoustic or optical) have positive frequencies at a zero pressure, which indicates the dynamic stability of these compounds. To determine the contribution of each atom to phonons, we have calculated the projected phonon density of states. From Fig. 4, it is evident that Zr atoms have a dominant contribution to forming acoustic branches (at frequencies as low as 200 cm^{-1}) whereas the contribution of cobalt

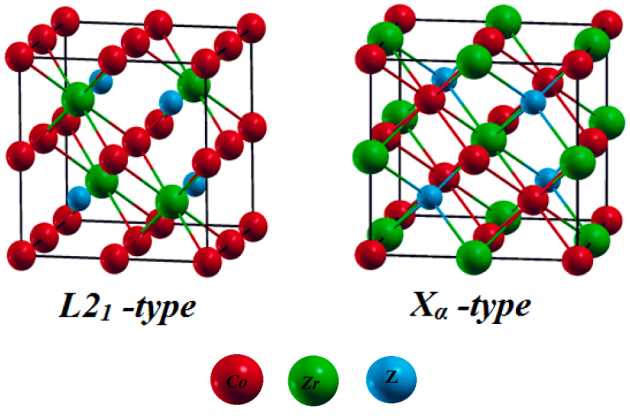

Fig. 1. Cubic Crystal structure of Co_2ZrZ (Z = Al, Si) full-Heusler alloys in $L2_1$- and X_α-type structures.

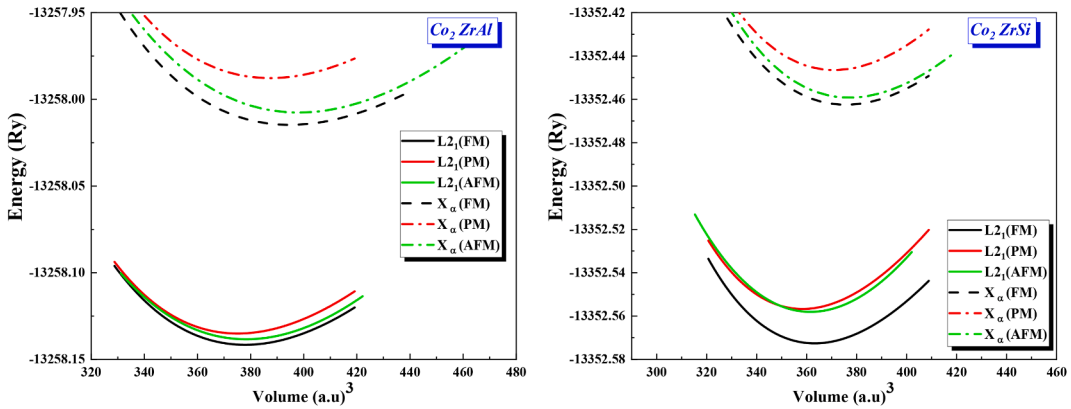

Fig. 2. The volume dependence of total energy for Co_2ZrAl and Co_2ZrSi compounds using GGA approximation in $L2_1$ and X_α-type structures.

Table 1
Calculated equilibrium lattice constants, bulk modulus, cohesive energy, Total and atomic magnetic moment of Co_2ZrZ (Z = Al, Si) Heusler alloys in both X_α and $L2_1$ phase structures using GGA approximation.

	Structural properties					Magnetic properties					
	Type		a(Å)	*B*(GPa)	E_{coh} (eV/atom)	$Co_{(1)}(\mu_B)$	$Co_{(2)}(\mu_B)$	$Zr(\mu_B)$	$Z(\mu_B)$	I zone (μ_B)	Tot (μ_B)
Co2ZrAl	X_α	AFM	6.179	135.58	5.391	1.270 −1.269 1.270 −1.270	1.522 −1.525 1.522 −1.525	−0.030 0.030 −0.030 0.030	−0.007 0.007 −0.007 0.007	−0.0009	0.00
		PM	6.123	145.19	5.325						
		FM	6.162	132.26	5.415	(4) 1.392	(4) 1.549	(4) −0.028	(4) 0.001	−0.061	2.852
	$L2_1$	AFM	6.075	162.76	5.836	0.856 −0.444 −0.444 −0.444	−0.878 0.455 0.455 0.455	0.000 0.000 0.000 0.000	0.000 0.000 0.000 0.000	0.009	0.00
		PM	6.058	167.43	5.825						
		FM	6.073	165.79	5.845	(4) 0.625	(4) 0.625	(4) −0.079	(4)−−0.01	−0.161	1.00
	Other work (theo)		6.05[33]			0.59[33]	0.59[33]	−0.10[33]	−0.0[33]		1.00[33]
Co_2ZrSi	X_α	AFM	6.068	155.41	5.758	1.060 −1.068 1.054 −1.068	1.314 −1.318 1.292 −1.318	−0.0147 0.0155 −0.0146 0.0152	−0.0146 0.0143 −0.0148 0.0143	−0.0006	0.00
		PM	6.036	166.91	5.708						
		FM	6.061	153.95	5.763	(4) 1.165	(4) 1.366	(4) −0.071	(4) 0.020	−0.114	2.365
	$L2_1$	AFM	5.984	197.18	6.087	1.017 −0.510 −0.510 −0.510	−1.021 0.511 0.511 0.511	0.0001 0.0001 0.0001 0.0001	0.000 0.000 0.000 0.000	0.002	0.00
		PM	5.966	190.41	6.083						
		FM	5.993	182.52	6.135	(4) 1.056	(4) 1.056	(4) −0.051	(4) 0.025	−0.088	2.00
	Other work (theo)		5.99[33]			1.04[33]		−0.07[33]	0.04[33]		2.00[33]

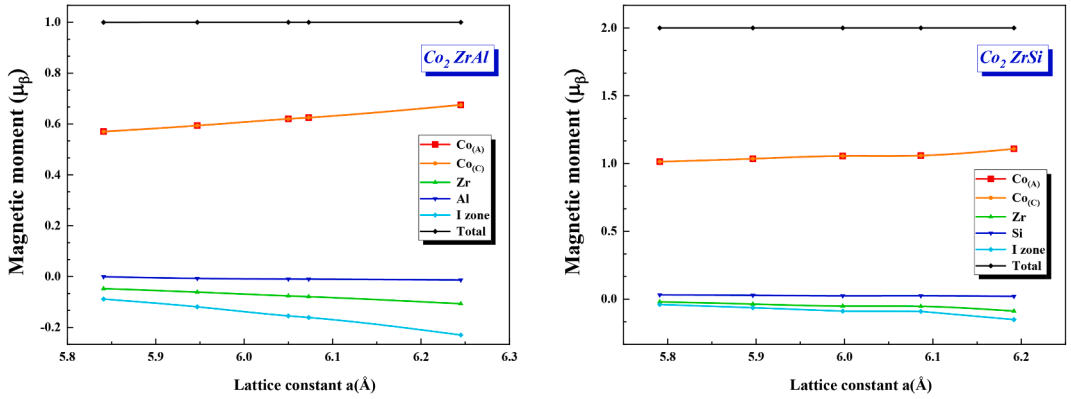

Fig. 3. Total and partial magnetic moment variations as function as lattice constant for Co_2ZrAl and Co_2ZrSi compounds using GGA approximation in $L2_1$-type structures.

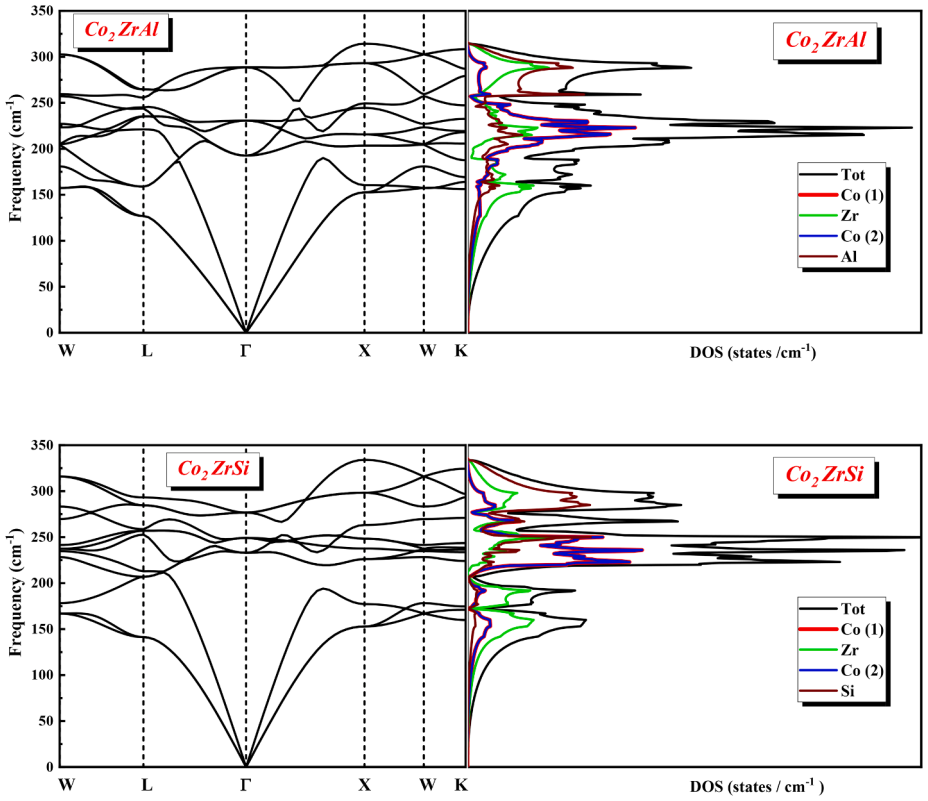

Fig. 4. Phonon band dispersion and phonon DOS of Co_2ZrAl and Co_2ZrSi Heusler compounds.

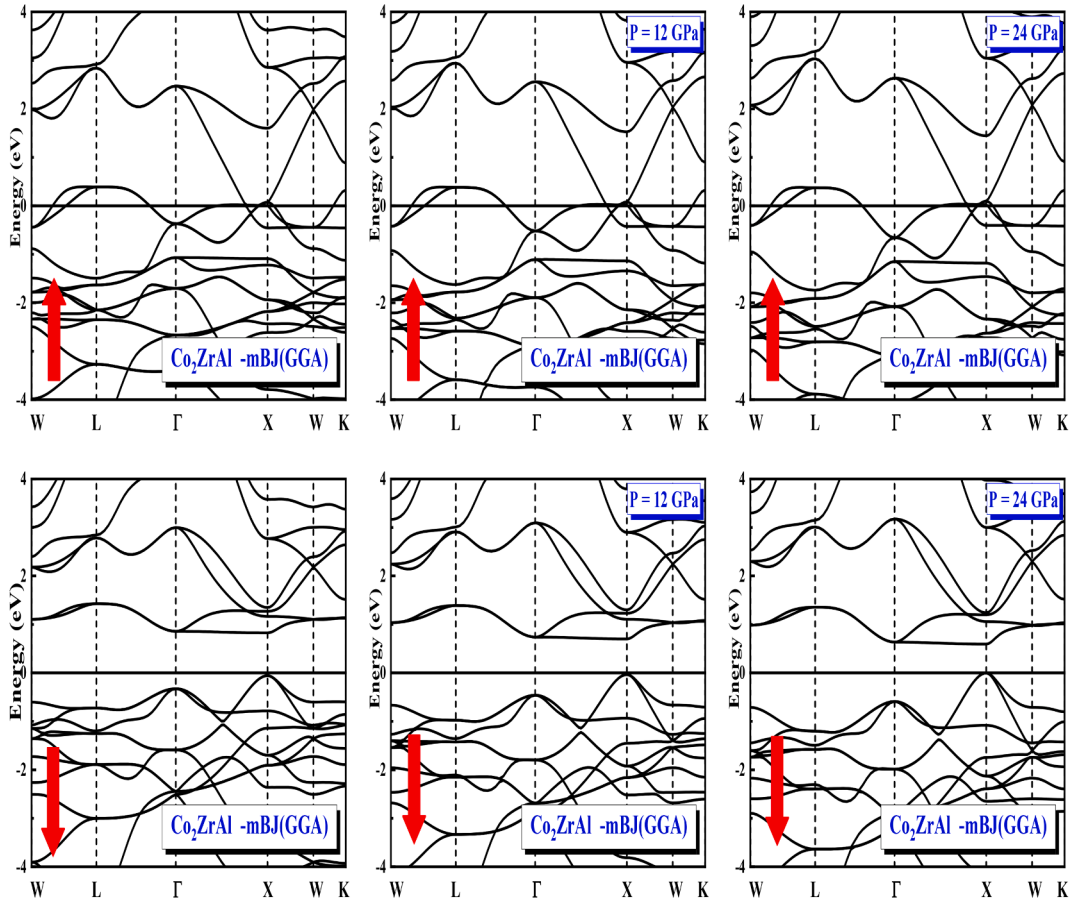

Fig. 5. Band structures for Co_2ZrAl compound using mBJ approximation calculated at different applied pressures (P = 0, 12 and 24 GPa).

atoms is dominant at frequencies between 200 and 250 cm^{-1}, and the contribution of light atoms(Al and Si) is at higher frequencies.

3.2. Electronic and elastic properties under pressure effect

Studying electronic properties is very important because it allows to classifying the material according to its nature and its electronic behavior to conductor, insulator, and semiconductor). Band structures, densities of states were chosen as analysis tools and the comparison between the curves of the band structures with the densities of states and the density states give us more information about how atomic orbitals contributing to the construction of these energy bands and to understand how bonds are formed between the atoms of this material. Also, we can use DOS and PDOS curves to explain how band gap can form and to explain the integer value of the total magnetic moment in Heusler alloys half metallic compounds and the Slater-Pauling rule.

The band structures calculated using mBJ approximation along high symmetry directions in the Brillouin zone are plotted in Figs. 5 and 6 at the equilibrium state (Pressure = 0 GPa) where we find that all the Heusler alloys studied in our work have band gaps in one spin direction, which confirmed the existence of the half-metallicity character. In the spin up direction, both Co_2ZrAl and Co_2ZrSi compounds exhibit an overlap between the valence and conduction bands as evidence of the metallic behavior of these compounds while in the down spin direction, we find that both conduction and valence bands are separated from each other by a direct band gap (X-X) of 0.88 eV for Co_2ZrAl indirect band gap (Γ-X) for Co_2ZrSi equal to 1.54 eV. The top of the valence band is at Γ and the bottom of conduction band is located at the X line, so both Co_2ZrAl and Co_2ZrSi compounds are semiconductors in spin-down channel and metals in the spin-up channel, this character called half metallicity.

Band gap in the half-metallicity Heusler alloys affects by the external strain, hence we want to check this effect under external strain. As an additional work, we have investigated the electronic behavior stability of the materials, and this by calculating the structures bands of Co_2ZrAl and Co_2ZrSi compounds without the influence of any pressure and also under the influence of pressures equal to 12 GPa and 24 GPa in both up and down spins channel (the results of our study are shown in Figs. 5-6 and Table.2). For spin up, there is no important change in our results compared to the stable state (0 GPa), whereas, when the Co_2ZrAl compound exposed to pressures 12 GPa and 24 GPa, the energy gap became direct (X-X) and decreased by 16.75% and 32.50% for pressures 12 GPa and 24 GPa, respectively. For Co_2ZrSi compound we recorded a slight change in the gap that does not exceed 5% when it exposed to a pressure equal to 24 GPa, and therefore we consider the second compound to be more stable in terms of electronic behavior.

The calculated total and partial density of states (DOS) using mBJ method for Co_2ZrAl and Co_2ZrSi Heusler alloys in the two spinal

Table 2
Energy bandgap (eV) for Co_2ZrAl and Co_2ZrSi compounds calculated at different applied pressures (P = 0 GPa, 12 GPa and 24 GPa).

	P = 0 GPa (equilibrium)		P = 12 GPa		P = 24 GPa	
	Spin up	**Spin down**	**Spin up**	**Spin down**	**Spin up**	**Spin down**
Co_2ZrAl	metal	0.883 (X–X)	metal	0.735 (X–X)	metal	0.596 (X–X)
Co_2ZrSi	metal	1.547 (Γ–X)	metal	1.553 (X–X)	metal	1.466 (X–X)

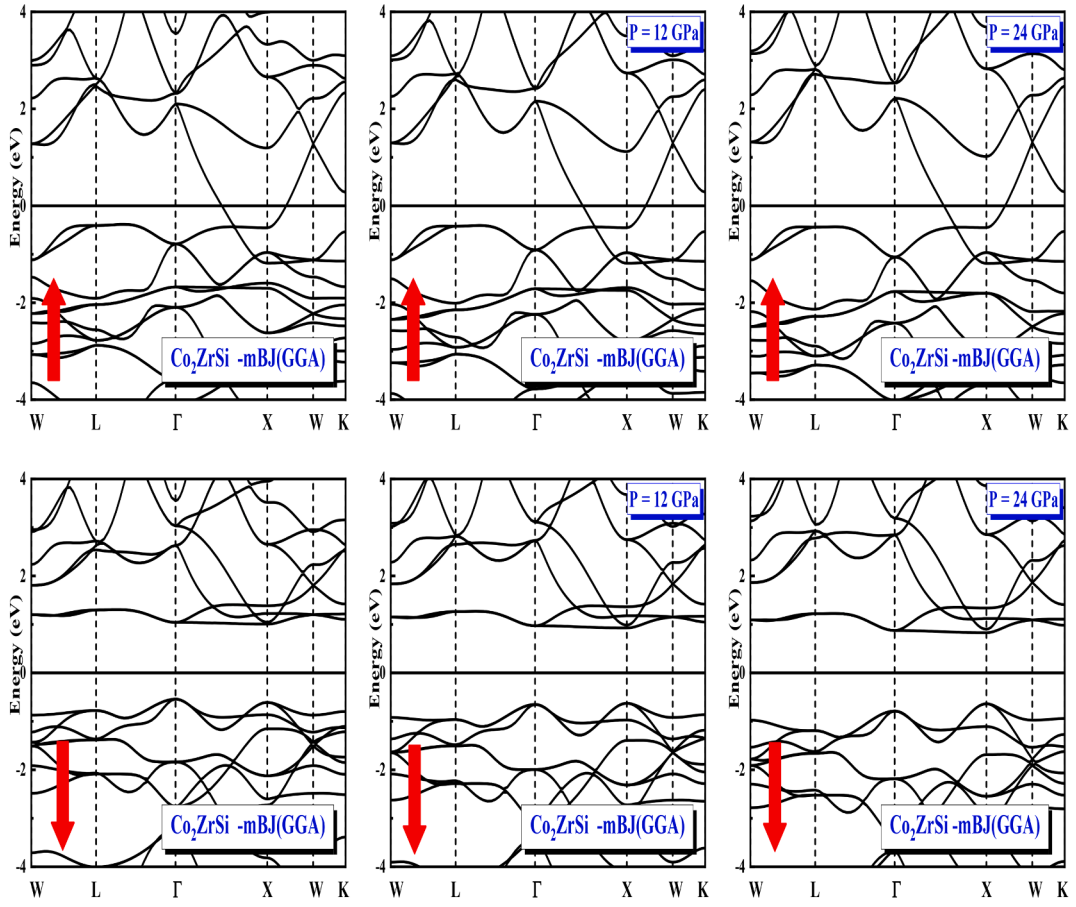

Fig. 6. Band structures for Co_2ZrSi compound using mBJ approximation calculated at different applied pressures (P = 0, 12 and 24 GPa).

directions (up and down) are plotted in Fig. 7. Both Co_2ZrAl and Co_2ZrSi Heusler alloys have band gaps in the spin-down channel, so we can easily see that for all studied alloys the majority spin band is metallic, while the spin-down band is a semiconductor with no density of states around Fermi level, which it proves the existence of half metallicity behavior in these alloys where our observation concerned the DOS shape curves is fully consistent with what was obtained when studying the domain structure of both compounds. This is the most important information that we have gone from the curves of the total density of states of these alloys. From DOS total curves we use $\rho\uparrow$ and $\rho\downarrow$spin projected density of states in the (up or down) spin state at the Fermi level (E_F) to calculate spin polarization (P) given by $P = \frac{(\rho\uparrow(E_F)-\rho\downarrow(E_F))}{(\rho\uparrow(E_F)+\rho\downarrow(E_F))}$ and it confirmed the half metallicity ferromagnetic nature of Co_2ZrAl and Co_2ZrSi alloys after we found that its value equal to 100% for all compounds which confirms the reported results.

We can get more detail about the atoms contribution through the projected density of states analysis which shows that the majority of density of states (PDOS) is mainly due to the strong d-d hybridization between the transition metal atoms. Also, a weak hybridization between p-d orbitals for Z (Al, and Si atoms) and Co atom. We notice that the 's', and 'p' states contributions of Co and Zr atoms are neglected compared to others. The distribution of the contributions of Z atom orbitals is as follows: 's' orbitals of Z atoms contributed in the region between (-6, −8eV for Co_2ZrAl and in (−8, −10 eV) for Co2ZrSi, and from (−6eV to −3 eV), we can see a week hybridization between p of Z atom and d orbital of Co. In spin down direction, the region from −6 to + 4 eV is mainly formed by Co-d and Zr-d states where Co-d states have a greater contribution than Zr-d in the region below Fermi level E_f for both compounds whereas Zr d-states contribution dominates the region above E_f. For both compounds in spin-down orientation, we can distinguish two regions comprising bonding (below E_f) and antibonding states (above E_f) states separating by band gap, both regions created mainly by the hybridization between of Co-d and Zr-d states with dominate of Co-d state.

In order to understand the origin of gap energy in the minority spin and the magnetic Slater Pauling rule of these compounds ($M_t = N_{ve}$-24), we analysis the effect of exchange splitting of the transition metal d states, This splitting in the electron atomic energy levels is due to the spin–orbit coupling interaction which is a relativistic interaction between electron spin magnetic moment with the magnetic field produced by the motion of the electron in the electrostatic field of the positively charged nucleus. For this reason, we plot in Fig. 7 total and partial density of states for both compounds and we concluded that the main contribution to the total magnetic moment is mainly due to Co d states with little contribution Zr-d states whereas the contributions of the s states of Z atoms very small and was positioned below d states of Co and Zr atoms and very far to Fermi level. For the p states of the Z atom, they hybridize with d orbitals the cobalt atoms to form Co-Z bonds. We can see from Fig. 5 that there is a strong hybridization of the d orbitals of the Co and Zr atoms near the Fermi level, so that the number of the resulting hybrid orbits is equal to the sum of the orbits involved in the hybridization process. Using the classical theory of molecular orbitals, we can explain the origin of the gap in two basic steps of hybridization shown in Fig. 8. The first hybridization occurs between Co and Zr atoms since the Zr atom is considered the first closest neighbor to Co, where d orbitals of Zr and Co atoms split in double degenerate d_{z2}, d_{x2-y2} and triple degenerate d_{xy}, d_{yx}, d_{zx} states, the double states of d_{z2}, d_{x2-y2} of Co atom can only couple with the same state of Zr (d_{z2}, d_{x2-y2}) atom and creating 2 bonding orbitals e_g and 2 other anti-bonding orbital e_u, meanwhile the

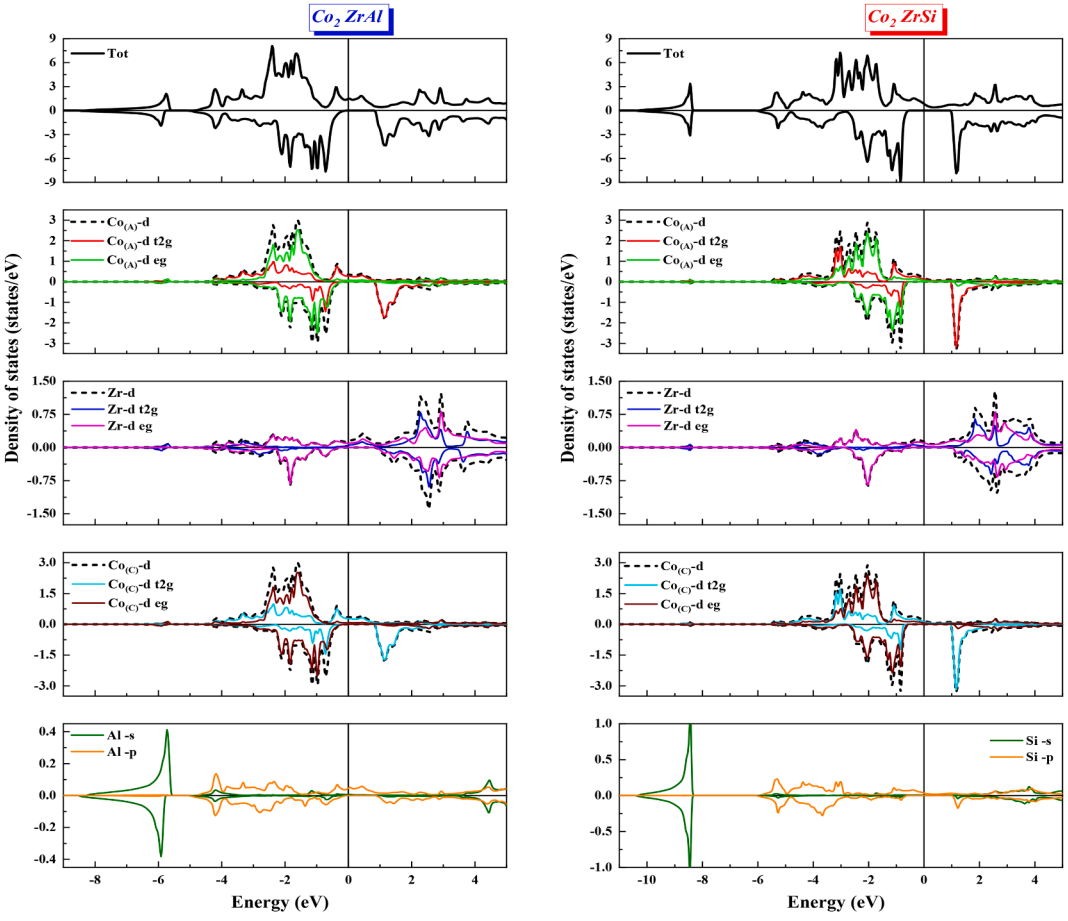

Fig. 7. Total and partial densities of Co_2ZrAl and Co_2ZrSi compounds with mBJ approximation at equilibrium lattice constant.

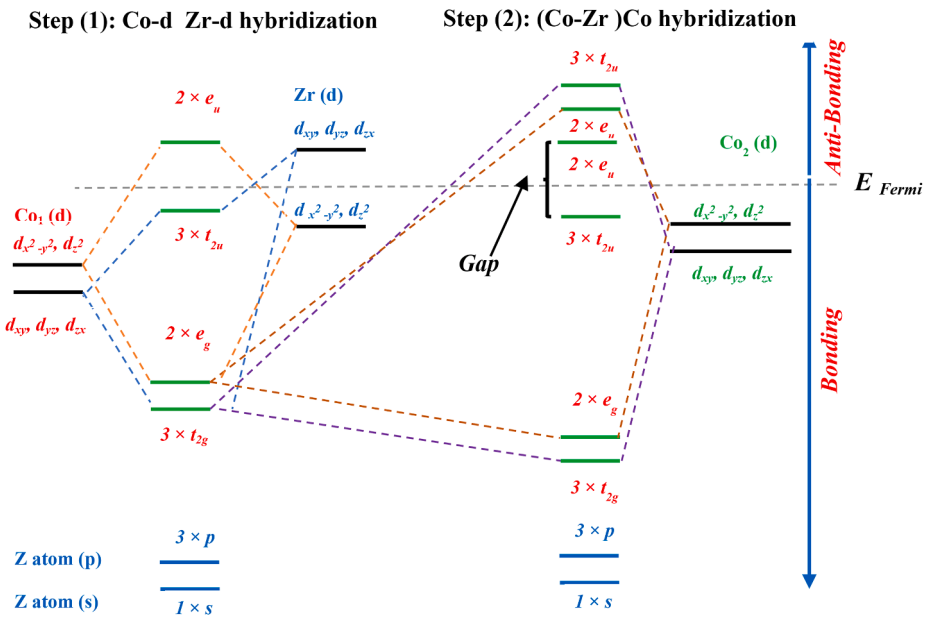

Fig. 8. Schematic illustration of the origin of the gap in the spin down of Co_2ZrZ Heusler alloys.

triple d_{xy}, d_{yx}, d_{zx} states of Co atom couple to d_{xy}, d_{yx}, d_{zx} of Zr atom forming 3 bonding t_{eg} and 3 antibonding orbitals t_u. As a second step, the hybrid orbitals resulting from the first hybridization (Co-Zr) enter into a second hybridization with the second cobalt atom, where the five anti-bonding (2 for e_u and 3 for t_{1u}) of Co orbitals cannot couple with any of the Co d-orbitals. The five bonding orbitals e_g and t_{eg} hybridize with the double states of d_{z2}, $d_{x2\text{-}y2}$ and the triple d_{xy}, d_{yx}, d_{zx} states Co atom respectively and it result again 5 bonding and 5 antibonding orbitals. The Fermi level is located below e_u and above t_{1u} orbitals, therefore, t_{1u} states are occupied unlike to e_u orbitals. From Fig. 6 one can see that there are 12 occupied ($1 \times s$, $3 \times p$, $2 \times e_g$, $3 \times t_{2g}$ and $3 \times t_u$) states below Fermi level in spin down direction and to occupy all we need 24 valence electrons shown in the magnetic Slater Pauling rule formula ($M_t = N_{ve} - 24$).

Co_2ZrAl as any other materials used in the industry undergoes to several factors influence, including pressure, which leads to deformation in their structures. The materials differ in their response to external forces due to their different structure's forces between the atoms, number and type of bonding between them and the space between atoms, therefore we can see different elastic properties such as stability, stiffness, hardness, rigidity and mechanically resistance…etc. In this work, we interested to investigate the elastic properties of $L2_1$-type structure for Co_2ZrAl and Co_2ZrSi Heusler alloys. Firstly, we calculated the three elastic constants C_{11}, C_{12} and C_{44} from the second-order derivatives of the fitted polynomials of the total energy, therefore C_{ij} constants have estimated during the calculation of the total energy as a function of volume-conserving strains that break the cubic symmetry, then, we computed several parameters such as bulk and shear modulus, Young's modulus (Y), Cauchy's pressure C'', Lamés' coefficients (λ and μ), Poisson's ratio (υ), Kleinman parameter (ξ) and anisotropy constant

Table 3
Calculated Elastic constants (C_{ij}), bulk modulus (B), Shear modulus (GV), Reuss shear (GR), Pugh's ratio (B/G), moduli of Young E, Cauchy's pressure (C"). Kleinman parameter (ξ), Poisson's ratio (υ), Elastic anisotropy (A), Frantsevich's ratio (G/B) and Lame's coefficients (μ and λ) of Co_2ZrZ (Z = Al, Si) Heusler alloys using GGA approximation under different pressure (P = 0 , 12 and 24 GPa).

		Co_2 ZrAl			Co_2 ZrSi		
		P = 0 GPa	**P = 12 GPa**	**P = 24 GPa**	**P = 0 GPa**	**P = 12 GPa**	**P = 24 GPa**
Elastic constants	**C_{11} (GPa)**	256.796	271.448	312.988	271.852	296.760	338.926
	C_{12} (GPa)	118.277	121.347	152.553	142.627	153.719	167.490
	C_{44} (GPa)	91.469	95.744	115.258	84.563	85.963	108.902
Bulk modulus	**B_V (GPa)**	164.450	171.380	206.031	185.702	201.399	224.635
	B_R (GPa)	164.449	171.381	206.032	185.702	201.398	224.637
	B_H (GPa)	164.449	171.380	206.031	185.702	201.398	224.636
Shear modulus	**G_V (GPa)**	82.584	87.466	101.241	76.583	80.186	99.628
	G_R (GPa)	81.070	86.233	98.114	75.267	79.538	98.270
	G_H (GPa)	81.827	86.849	99.677	75.925	79.862	98.949
Young modulus	**Y_V (GPa)**	212.226	224.248	260.976	201.983	212.372	260.388
	Y_R (GPa)	208.884	221.541	254.019	198.925	210.856	257.291
	Y_H (GPa)	210.557	222.895	257.504	200.455	211.614	258.841
Poisson's coefficient	**P_V**	0.284	0.281	0.288	0.318	0.324	0.306
	P_R	0.288	0.284	0.294	0.321	0.325	0.309
	P_H	0.286	0.283	0.291	0.320	0.324	0.307
Lamés' coefficients	**λ**	109.393	113.070	138.537	134.647	147.942	158.216
	μ	82.585	87.466	101.241	76.582	80.186	99.628
Kleinman parameter	**ξ**	0.591	0.579	0.614	0.645	0.640	0.620
Anisotropy ratio	**A (s.u)**	1.320	1.280	1.440	1.310	1.200	1.270
Cauchy's pressure	**C'' (GPa)**	26.808	25.603	37.295	58.064	67.756	58.588
Pugh's ratio	**B/G**	2.009	1.973	2.066	2.445	2.521	2.270

(A). the obtained results using Voigt Reuss Hill approximations (VRH) [37–39] are summarized in Table 3. We note that to date, no experimental or previous theoretical results are available to be compared with our obtained results. The mathematical relationship between the elastic constants and each of these elastic parameters are given as following [40]:

$$B = \frac{1}{3}(C_{11} + 2C_{12}) \tag{3}$$

$$G_V = \frac{C_{11} - C_{12} + 3C_{44}}{5} \tag{4}$$

$$Y = \frac{9BG_v}{3B + G_v} \tag{5}$$

$$A = \frac{2C_{44}}{C_{11} - C_{12}} \tag{6}$$

$$C^{''} = (C_{12} - C_{44}) \tag{7}$$

$$v = \frac{3B - E}{6B} \tag{8}$$

$$\xi = \frac{C_{11} + 8C_{12}}{7C_{11} + 2C_{12}} \tag{9}$$

$$\lambda = \frac{Yv}{(1+v)(1-2v)} \tag{10}$$

$$\mu = \frac{Y}{2(1+v)} \tag{11}$$

Analysis of the elastic properties results starts from the elastic constants C_{ij}, where we can see that the obtained values satisfy the mechanic Born-Huang mechanic stability criteria [41] for both Co_2ZrAl and Co_2ZrSi ((C_{11} + 2 C_{12}) > 0, C_{11}, C_{12} and C_{44} greater than 0, (C_{11}-C_{12}) > 0. The bulk modulus (*B*) describes how a material reacts when it is compressed uniformly, the results obtained by using Voigt Reuss-Hill approximations gave very similar results. The Co_2ZrSi compound has a greater coefficient of compressibility than the other once, and thus its resistance to external pressure is greater. Obviously, for both compounds, Co_2ZrAl and Co_2ZrSi, the bulk moduli calculated from elastic constants are in good agreement with those provided by the EOS Eqs. (Table 1). We can study rigidity of any materials through the shear modulus (G) values and in contrast to bulk modulus. We found that the shear modulus Co_2ZrAl is greater than Co_2ZrSi. Dividing bulk modulus to shear modulus is called the Pugh's ratio [42], as this ratio refers to the nature of the material: ductile if (B/G) greater than 1.75 and brittle in the reverse case. Pugh's ratio values obtained indicate that they possess ductile nature with high malleability. As shown in Eq. (7) Cauchy's pressure estimated by the difference between C_{12} and C_{44}, can be used to get an idea about the kind of bonds for a compound, if C_{12} smaller than C_{44} (C" is negative), mostly the bond dominate is covalent , otherwise, it is ionic bonds. Consequently, the Cauchy's pressure calculated for both compounds has a positive sign, hence the bonds in both compounds are ionic. We can also assess the nature of the bond through another indicator which is Poisson's ratio, this latter expresses the behavior of any compound when it compressed in one direction, it expands in the other two directions perpendicular to the direction of compression. Another benefit that can be obtained from knowing the value of the Poisson rate is related to the nature of the bonds between the atoms where for typical covalent bonding its value around 0.1 whereas for typical ionic crystals up to 0.25. So according to our results, Poisson's coefficients are greater than 0.25, thus the bond dominated for both compounds is ionic.

As a feature from the elastic properties of materials, we studied the ability to resist any change in length when the material obeyed to a longitudinal stretching or compression process in one direction. This feature was calculated by mathematical Eq. (8) and named Young's modulus, and the detailed results in Table 3 implies that Co_2ZrAl compound has a greater longitudinal expansion ability than Co_2ZrSi compound.

Anisotropy of a material is another important parameter, which determined whether the properties of the alloys are the same in all directions or not when a material undergoes to uniform stress. If Anisotropy equal to unity, crystal consider as isotropic, other values greater or smaller than unity its properties change along with different directions. Our results hint that both compounds are anisotropic. Both of λ and μ Lame's parameters have calculated using Eqs. (10) and (11) formula respectively, where λ determined the compressibility of the material, and μ its shear stiffness. Co_2ZrAl Heusler alloys compared to Co_2ZrSi has greater shear coefficient and smaller compressibility factor. Kleinman parameter (ξ)[43] calculated using Eq. (9) computes the internal strain, knowing its value helps us to determine which type of bond is dominate (stretching or bending bonds). Thus, we can know the general nature of the internal bonds, if they are stretching or bending and according to the type of the predominant bond, the compound will exhibit two different behaviors either elongation or distortion. According to the obtained values for the Kleinman parameter, we can see that bond nature is dominated by the bond stretching term in both Co_2ZrAl and Co_2ZrSi Heusler alloys.

Studying of the aforementioned elastic characteristics under uniform pressure effect was calculated again at both pressures 12 GPa and 24 GPa and was summarized in Table 3, where we can easily observe an increase in the most properties with the increase of pressure such as the elastic constants, bulk and shear modulus, Young moduls and Lamés' coefficients…….etc. with an increase in pressure for both Co_2ZrAl and Co_2ZrSi Heusler alloys.

3.3. Thermodynamic and thermoelectric properties

The calculations obtained by using the wien2k program are performed at zero temperature, meaning that we neglected the vibrational side of the atoms in the hamiltonian equation of the crystal system with a view to simplify the Schrödinger equation and this was via applying the Born-Oppenheimer approximation [36]. For this reason, the effect of temperature also the thermal properties are investigated using the quasi-harmonic model [44] implemented in GIBBS2 code [45,46].

The function controlling the phase stability of a solid at a given pressure and temperature is the Gibbs free energy given by:

$$G^*(x, V; P, T) = E_{sta}(x, V) + PV + A^*_{vib}(x, V; T) + F^*_{el}(x, V; T) \tag{12}$$

where E is the total energy, PV corresponds to the hydrostatic condition, A^*_{vib} and $F^*_{el}$are the non-equilibrium vibrational and electronic free energies respectively. Debye's model is used to write the vibrational energy A^*_{vib}in terms of the density of phonon states (the vibrational density of states) g(ω):

$$A^*_{vib} = \int_0^{\infty} \left[\frac{\omega}{2} + k_B T \mathrm{Ln}(1 - e^{-\frac{\omega}{k_B T}})\right] g(\omega) d\omega \tag{13}$$

$$F^*(x, V; T) = E_{sta}(x, V) + A^*_{vib}(x, V; T) \tag{14}$$

In this equation, n is the number of atoms per unit volume, D (θ / T) represents the Debye integral which is written by:

$$D(x) = \frac{3}{x^3} \int_0^x \frac{y^3 e^{-y}}{1 - e^{-y}} dy \tag{15}$$

The equilibrium state (for pressure (P) and a temperature (T) given) is obtained by the minimization of:

$$\left(\frac{\partial G^{*}(V,P,T)}{\partial V}\right)_{P,T} = 0 \tag{16}$$

Resolving Eq. (16) makes it easy to express the other thermal quantities in particular: entropy (S), the heat capacity at constant volume (C_v), and the coefficient of thermal expansion which are expressed:

$$S = -3nk_B\ln\left(1 - e^{-\Theta_D/T}\right) + 4nk_B D(\Theta_D/T) \tag{17}$$

$$C_v = 12nk_B D(\Theta_D/T) - \frac{9nk_B\Theta_D/T}{e^{\Theta_D/T} - 1} \tag{18}$$

$$\alpha = -\frac{1}{V}\left(\frac{\partial V}{\partial T}\right)_P = \frac{YC_v}{VB_T} \tag{19}$$

The temperature effect on heat capacities at volume and pressure constant, entropy, Debye temperature, thermal expansion and thermal conductivity in the temperature range of 0–1000 K are shown in Fig. 8.

For Co_2ZrZ (Z = Al, Si) Heusler alloys, the heat capacity (see Fig. 9-a) at volume constant checked the law of Petit Dulong at high temperatures [47] at high temperature where its value reached to 100 (J/mol. K) when the temperature is greater than 550 k, while C_v is proportional to T^3 at low temperature, meanwhile, we can see that heat capacity (see Fig. 9-b) at pressure constant has the similar behavior to C_v capacity.

The variation of the coefficient of thermal expansion (α) as a function temperature is shown in Fig. 9-c. According to this figure, we can be seen that the thermal expansion increases very rapidly for temperatures smaller than 250 K, and it increases slowly with temperatures greater than 250 k and becomes almost linear. Also, we can see that at high-temperature Co_2ZrSi has high value compared to Co_2ZrAl. Fig. 9-d appears that the entropy increases with the increase of the temperature because the increase of the temperature leads to a growth of the modes of vibration and consequently the number of configurations possible. We note that there is no significant difference between the two components studied for the entropy values.

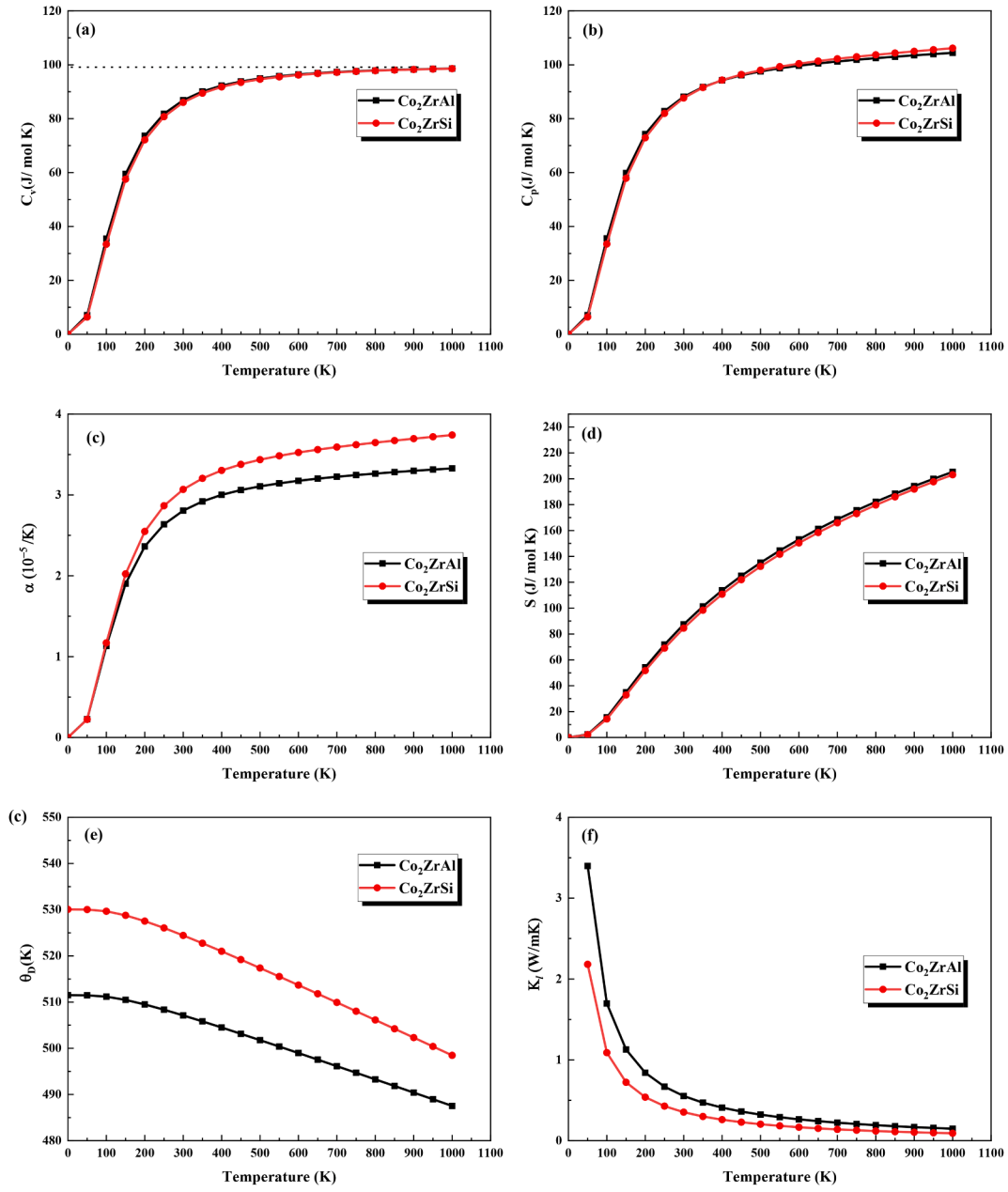

Fig. 9. Variation of heat capacities (C_V and C_p), entropy (S), thermal expansion (α), Debye temperature (θ_D) and crystal conductivity (K_l) of Co_2ZrAl and Co_2ZrSi Heusler alloys as a function of temperature.

Debye temperature is the most important thermal property, it is associated with many mechanical and elastic properties and it represents the corresponding temperature which caused the highest possible number of modes vibration. Through Fig. 9-e, we note that the temperature of Debye varies inversely with the change in temperature. It can also be observed that the temperature of Debye in Co_2ZrSi is greater than Co_2ZrAl at high temperature.

In order to know the distribution of the contributions of phonons in the thermal conductivity, we studied in Fig. 9-f the changes in crystal conductivity K_l for Co_2ZrSi and Co_2ZrAl Heusler alloys in terms of temperature. The k_ℓ can be calculated using the Slack model formula given by [48]:

$$K_l = \frac{A\vartheta_D{}^3 V^{1/3} m}{\gamma^2 n^{2/3} T} \tag{20}$$

where A is a physical constant equal to $A = \frac{2.4310^{-8}}{1-\frac{0.514}{\gamma}+\frac{0.228}{\gamma^2}}$ and θ_D, γ, V, n and m are the Debye temperature, Grüneision parameter, the volume per atom, the number of atoms in the primitive unit cell and m is the average mass of all the atoms in the crystal respectively). For Co_2ZrZ (Z = Al, Si) Heusler alloys, Fig. 9-f shown that K_l exponentially decreases with the increasing temperature and it reaches its lowest level when the temperature is in a range greater than 500 K while at lower temperatures the conductivity for Co_2ZrSi compound is much greater than the other compound.

Heat capacity of metals is significant because it expresses the ability of a substance to absorb energy. This ability logically increases with the increasing number of degrees of freedom of particles. Entropy on a microscopic scale can be defined as a measure of the disorder of a system, and it is viewed as a measure of the number of possible configurations. As the temperature rises, the atoms start to oscillate, then new configurations become possible. The influence of pressure on the behavior of heat capacity C_v and entropy at room temperature equal to 300 K is shown in Fig. 10-a and -b. one can observe that for Co_2ZrZ(Z = Al, Si) Heusler alloys both heat capacity C_V and entropy S decrease linearly with the increase in pressure because the increase in pressure affects the movements of atoms and therefore decreases vibration modes. Unlike C_v and S properties, the thermal conductivity K_l increases with increasing pressure (see Fig. 10-c), this can be explained by the decreasing of interatomic distances. Also, we can see that at ambient temperature (300 K) Co_2ZrSi has a higher value of entropy, heat capacity and thermal conductivity compared to Co_2ZrAl.

Based on semi-classical Boltzmann transport theories implemented in BoltzTraP code [29] we investigated different transport coefficients Co_2ZrAl and Co_2ZrSi Heusler alloys such as Seebeck coefficient (S), electrical conductivity (σ/τ), Thermal conductivity (κ/τ), the figure of merit (ZT), electronic specific heat capacity (c) and Pauli magnetic susceptibility (χ) in the constant relaxation time approximation as a function of μ (Fermi level energy) in the temperature range from 300 to 1000 K for both spin's directions. We only plotted the variations of these coefficients at three temperature degrees 300, 500 and 700 K. We note that there are no previous studies on thermoelectric properties for Co_2ZrSi Heusler alloys.

The Seebeck effect is an intrinsic property of a material and it expresses the ratio of the voltage generated between the ends of a material when exposing its ends to the temperature gradient. This temperature difference results in the moving charge carriers (electrons or holes) moving and induced an electrical current.

We plotted in Fig. 11-a the variation of Seebeck coefficient along the relative chemical potential μ to the Fermi level μ_0 in both spin directions where the values of μ_0 are 0.735 Ry, 0.821 Ry for Co_2ZrAl and Co_2ZrSi respectively. We can see from Seebeck coefficient curves that in spin-up Seebeck coefficient value is almost negligible compared to the spin-down. In spin down case, Seebeck coefficient (S) reaches a maximum at 300 K for Co_2ZrAl and Co_2ZrSi compounds and decrease with the increasing of temperature. Co_2ZrSi in spin-down direction has a

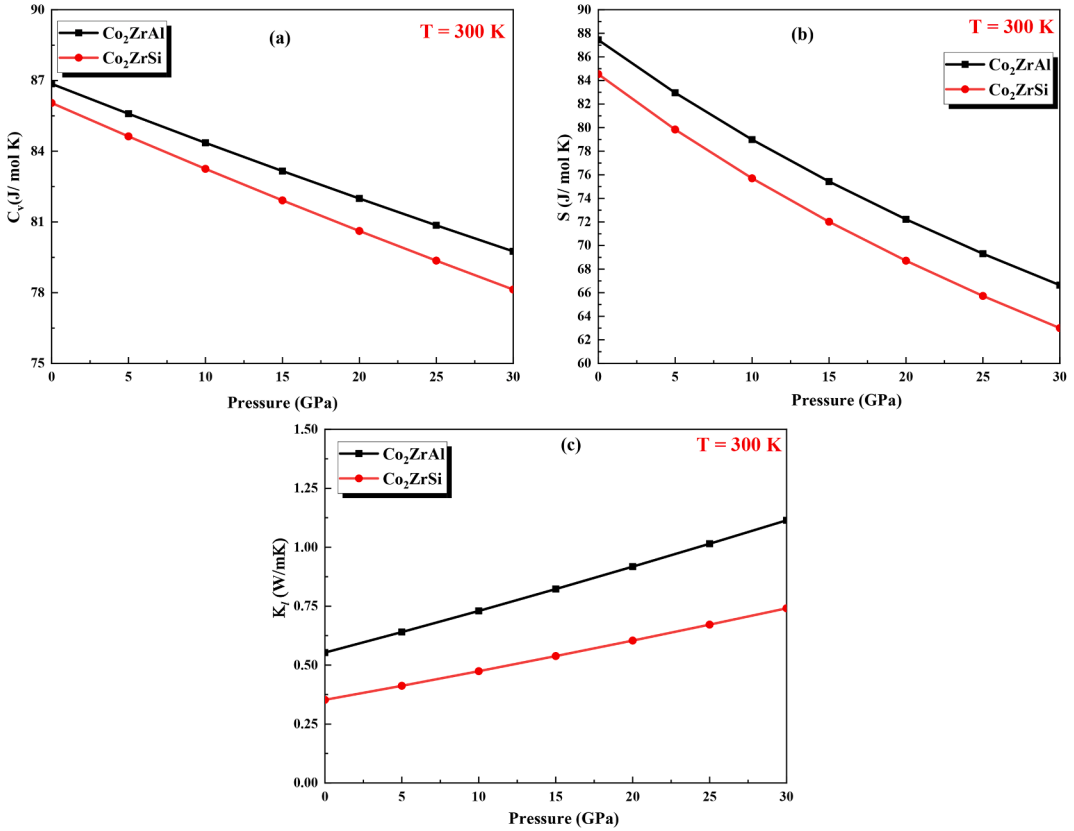

Fig. 10. Variation of heat capacity (C_V)entropy (S) and crystal conductivity (K_l) of Co_2ZrAl and Co_2ZrSi Heusler alloys as a function of pressure.

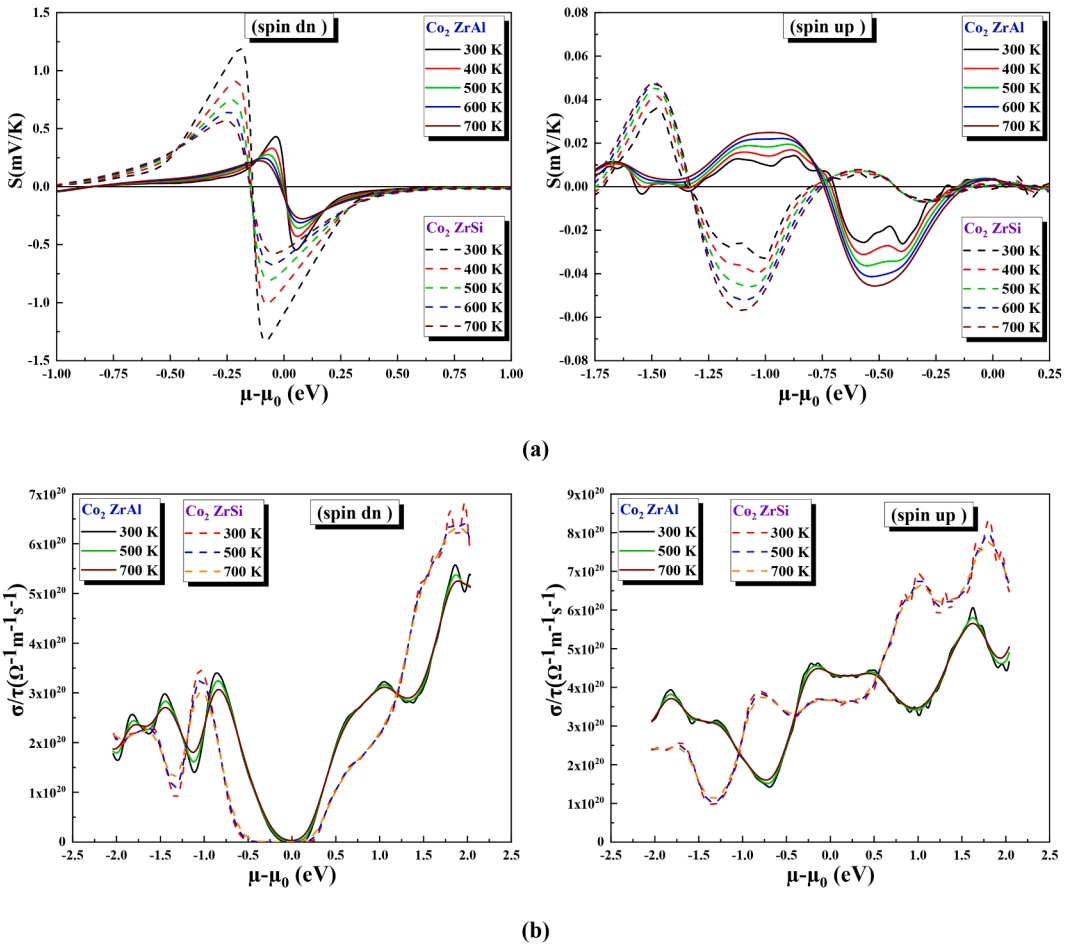

Fig. 11. Variation of thermoelectric coefficient as function as chemical potential of Co_2ZrAl and Co_2ZrSi Heusler alloys in both spin directions: (a) Seebeck coefficients, (b) electrical conductivity.

maximum value of Seebeck coefficient reached to 1.25 mV/K and has a higher coefficient value than other alloys which indicates that this material has a good thermoelectric performance.

Electrical conductivity expresses the ability of a material to conduct electric current, its value related to the mobility of the charge carriers (holes and electrons) and the carrier concentrations in materials. We use the electrical conductivity (σ/τ) coefficient to describe the contribution of the free electrons in Co_2ZrAl and Co_2ZrSi alloys in conductivity, so its variation in terms of chemical potential in temperature range are shown in Fig. 11-b.Through these curves, we can see similar shapes of curves for all temperatures and the electrical conductivity has a maximum between 1.5 and 2.0 eV for all compounds in both spins up and down directions and we can observe that Co_2ZrSi has a greater electrical conductivity that Co_2ZrAl in the relative chemical potential range between 1.5 and 2 eV. There is no electrical conductivity around the Fermi level in spin-down direction for both compounds.

We plotted in Fig. 12 (a, b and c) the electronic thermal conductivity (κ/τ), electronic specific heat (c) and Pauli magnetic susceptibility (χ) as a function of chemical potential. The thermal conductivity is the sum of the electronic (κ_e) and lattice (κ_l) conductivities contributions ($\kappa = \kappa_e + \kappa_l$). To get a good material used for converting heat to an electrical courant, It's enough to be the electronic conductivity higher than lattice conductivity, when two sites in the material are exposed to two different temperature grades, the ratio of the movement of electrons is higher than the ratio of vibration of the atoms in the lattice; hence we can see current of electrons instead phonons vibrations. From Fig. 12-a, we can see that in the spin-down direction the lowest values of the thermal conductivity were in the region of the chemical potential relative near to the Fermi level for all temperature for both Heusler compounds. In spin up and down direction the thermal conductivity has a higher value in positive relative potential compared to the negative range in all temperatures. Also, we can observe that the electronic thermal conductivity (κ/τ), increase with the increase of temperature. Regarding the shape of both thermal and electrical conductivity curves, we note that thermal conductivity has similar behavior to electrical conductivity for all compounds in both spin orientations. This confirms that the transfer of electrons contributed to the transfer of heat where the thermal conductivity is proportional to the electrical conductivity, and this relationship follows to a Wiedemann–Franz law given by:

$$K_e = L\sigma T(whereLisLorenteznumber) \tag{21}$$

The transfer of heat in solid materials depends on the contribution of both free electrons and phonons (the vibration of the atoms), so that the capacity of each of them differs in the transfer of heat according to the nature of the metal (pure or impurities). Electron heat capacity is reduced when the ratio of impurities increases which impedes the movement of a free-electron through collisions that lose its transport energy. The variation of the electronic heat capacity (c) as function as the relative chemical potential at different temperatures in both up and down spin directions of Co_2ZrAl and Co_2ZrSi Heusler alloys are shown in Fig. 12-b. We note through these figures that in the case of spin-down, the electronic heat capacity has small values around Fermi level, and it increases with both the chemical potential and temperature on the positive side. In spin-up, electronic heat capacity takes up different values as long as the chemical potential range studies (whether it has positive or negative values, its value increases with increasing

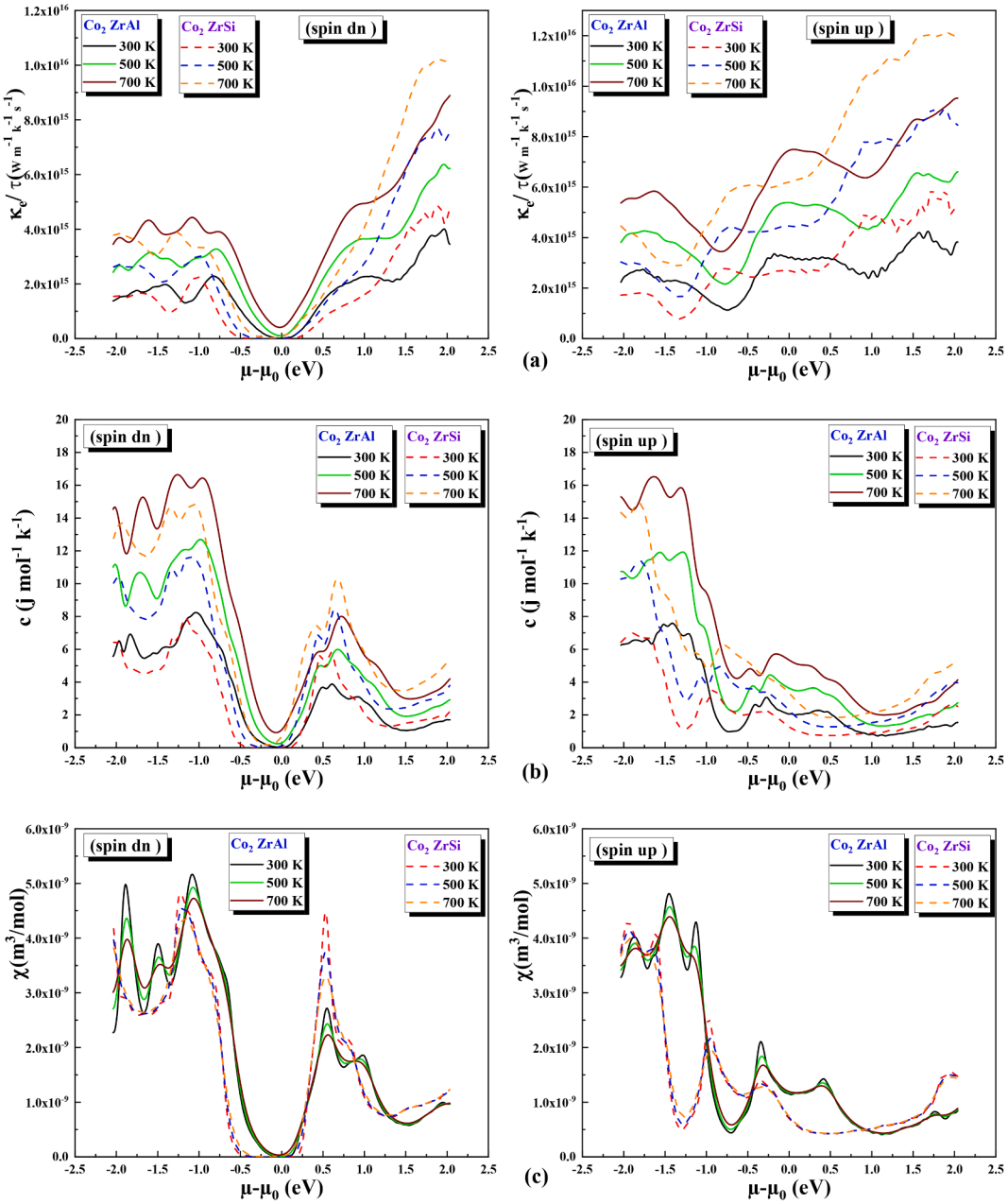

Fig. 12. Variation of thermoelectric coefficient as function as chemical potential of Co_2ZrAl and Co_2ZrSi Heusler alloys in both spin directions: a) electronic thermal conductivity, (b) electronic specific heat and (c) Pauli magnetic susceptibility.

temperature. According to the Wiedemann–Franz law, which relates thermal conductivity and electrical conductivity of free electrons, therefore, to select ideal materials used in heat-electrical converting devices we need to increase thermal conductivity to obtain high electrical conductivity.

Pauli magnetic susceptibility (χ) describes the behavior of conduction electrons when exposed to an external magnetic field. Fig. 12-c shown the variation of Pauli magnetic susceptibility (χ) calculated at 300, 500 and 700 K temperatures as function as relative chemical potential. This latter coefficient in spin-down was zero for all temperature when the relative chemical potential was between −0.5 to 0.25 eV for Co_2ZrSi and −0.25 to 0.2 eV for Co_2ZrAl the highest value of Pauli magnetic susceptibility (χ) has found in the negative part of the relative chemical potential (the maximum was around −1 eV for both compounds).

Fig. 13-a display the figure of merit ZT which it expresses the qualification of materials to transfer heat into useful electric energy for Co_2ZrAl and Co_2ZrSi Heusler alloys as a function of chemical potential at different temperatures. Thus, materials have a higher ZT have higher efficiency when we use thermoelectric devices. From Fig. 13-a we can see that ZT takes higher values for relative chemical potential between −0.5 to −0.25 eV and from 0.25 to 0.5 eV in spin-down direction while between these two ranges ZT has zero value. In addition, the ZT value decreases with increasing temperature and Co_2ZrSi is greater than the other alloys, meanwhile; ZT ratio in majority spin has almost negligible value for both compounds.

Power factor $P = S^2.\sigma$ is calculated for Co_2ZrAl and Co_2ZrSi Heusler alloys and the obtained results plotted in both spins arrangement at different temperatures as function as the chemical potential and plotted in Fig. 13-b, through these curves we can see that Power factor increases when the temperature increase in both spin directions for all compounds, also Fig. 13-b displays that the maximum power factor around

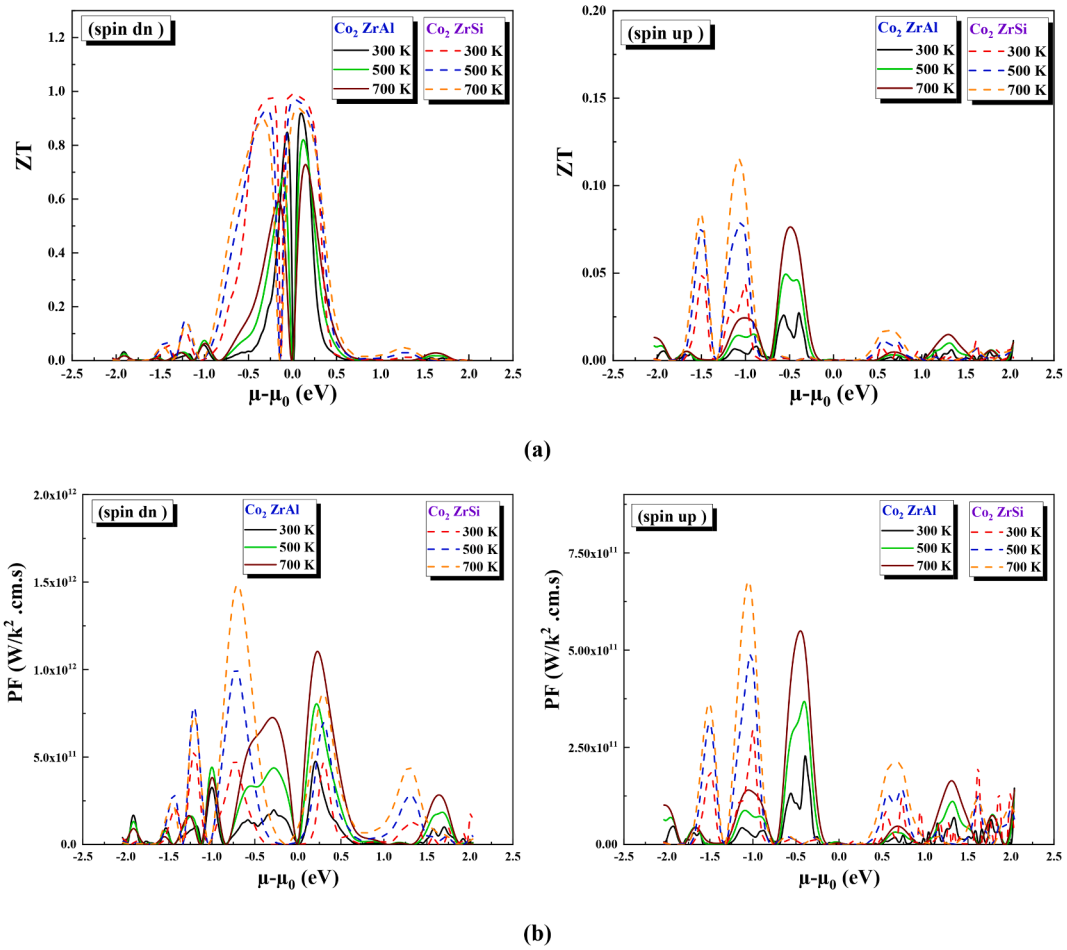

Fig. 13. Variation of thermoelectric coefficient as function as chemical potential of Co_2ZrAl and Co_2ZrSi Heusler alloys in both spin directions: (a) the merit (*ZT*) and (b) power factor P.

μ-$\mu_0 = 0.25$ eV for Co_2ZrAl in spin down and -0.75 eV for Co_2ZrSi where Co_2ZrSi gives high values compared to Co_2ZrAl.

Temperature effect on electronic thermal conductivity for Co_2ZrAl and Co_2ZrSi Heusler alloys is plotted in Fig. 14 Where Ke appears to increase linearly with increasing temperature in spin up direction. For the spin-down case, the electronic conductivity is almost neglected compared to Spin-up arrangement. Through the figure, it becomes clear that the electronic conductivity value is non-existent when the temperature is less than 300 K for Co_2ZrAl and less than 400 K for Co_2ZrSi. When the temperature rises above the two mentioned values, the electronic conductivity begins to increase exponentially with the increasing temperature. This difference is mainly due to the nature of the materials in each spin direction where we find that in spin up the material behaves like a metal and the movement of free electrons of conducting is easier and faster than the vibrations of the atoms Hence electron motion carries thermal energy while in the case of the semiconductor it is more difficult and complicated.

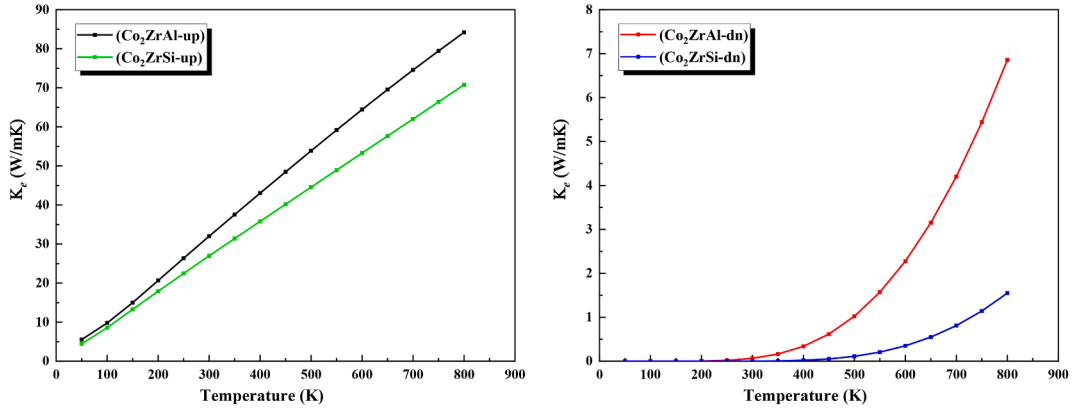

Fig. 14. Temperature dependence of ecteronic thermal conductivity K_e Co_2ZrAl and Co_2ZrSi Heusler alloys.

4. Conclusion

Using first-principles calculations, we found that Co_2ZrAl and Co_2ZrSi components are more stable in structure $L2_1$ phase structure in ferromagnetic state with integer values of total magnetic moments that fulfill the Slater Pauling principle. Also, both compounds verified the dynamic stability criterion where we found that all the frequencies of the acoustic and optic phonon branches were positive.

The total magnetic moment under the influence of pressure was calculated and the results show that its value not changes. The calculated lattice and electronic thermal conductivities refer to that electronic contribution is more dominant than the lattice contribution at high temperatures. The obtained thermoelectric coefficient indicates that Co_2 based Heusler alloys are good candidate thermoelectric due to their high electrical conductivity, high Seebeck coefficient reached 1.25 mV/K for Co_2ZrSi and low thermal conductivity values. The elastic properties under pressure effect were also determined, and the findings point out that the properties did not change significantly, especially in the Co_2ZrSi compound.

CRediT authorship contribution statement

S. Sâad Essaoud: Conceptualization, Methodology, Data curation, Software, Writing - original draft. **Ahmed S. Jbara:** Writing - review & editing.

Declaration of Competing Interest

The authors declare that they have no known competing financial interests or personal relationships that could have appeared to influence the work reported in this paper.

References

[1] I.M. Abdel-Motaleb, S.M. Qadri, Thermoelectric devices: principles and future trends, ArXiv Prepr. ArXiv170407742 (2017).
[2] F. Heusler, Über magnetische manganlegierungen, Verhandlungen Dtsch. Phys. Ges. 5 (1903) 219.
[3] S.B. Riffat, X. Ma, Thermoelectrics: a review of present and potential applications, Appl. Therm. Eng. 23 (2003) 913–935.
[4] L.E. Bell, Cooling, heating, generating power, and recovering waste heat with thermoelectric systems, Science. 321 (5895) (2008) 1457–1461.
[5] G.J. Snyder, E.S. Toberer, Complex thermoelectric materials, in: Mater. Sustain. Energy Collect. Peer-Rev. Res. Rev. Artic. Nat. Publ. Group, World Scientific, 2011: pp. 101–110.
[6] H. Osterhage, J. Gooth, B. Hamdou, P. Gwozdz, R. Zierold, K. Nielsch, Thermoelectric properties of topological insulator Bi_2Te_3, Sb_2Te_3, and Bi_2Se_3 thin film quantum wells, Appl. Phys. Lett. 105 (2014), 123117.
[7] B.T. Miller, L. Hug, T. Helbling, Potential of Thermoelectrics for Waste Heat Recovery, (n.d.).
[8] H.Y. Lee, J.K. Lee, Dissolution of Thermoelectric Materials Containing Te with Acidic Solutions, Sep. Sci. Technol. 50 (11) (2015) 1665–1670.
[9] H. Shi, D. Parker, M.-H. Du, D.J. Singh, Connecting Thermoelectric Performance and Topological-Insulator Behavior:Bi_2Te_3 and Bi_2Te_2Se from First Principles, Phys. Rev. Appl. 3 (2015).
[10] K. Kaur, D.P. Rai, R.K. Thapa, S. Srivastava, Pursuit of thermoelectric properties in a novel Half Heusler compound: HfPtPb, ArXiv Prepr, ArXiv170504015. (2017).
[11] T. Jaeger, C. Mix, M. Schwall, X. Kozina, J. Barth, B. Balke, M. Finsterbusch, Y. U. Idzerda, C. Felser, G. Jakob, Epitaxial growth and thermoelectric properties of TiNiSn and Zr0.5Hf0.5NiSn thin films, Thin Solid Films. 520 (3) (2011) 1010–1014.
[12] K. Mastronardi, D. Young, C.-C. Wang, P. Khalifah, R.J. Cava, A.P. Ramirez, Antimonides with the half-Heusler structure: New thermoelectric materials, Appl. Phys. Lett. 74 (10) (1999) 1415–1417.
[13] S. Yousuf, D.C. Gupta, Thermoelectric and mechanical properties of gapless Zr_2MnAl compound, Indian J. Phys. 91 (1) (2017) 33–41.
[14] T. Fang, X. Zhao, T. Zhu, Band structures and transport properties of high-performance Half-Heusler thermoelectric materials by first principles, Materials. 11 (2018) 847.
[15] A. Abada, K. Amara, S. Hiadsi, B. Amrani, First principles study of a new half-metallic ferrimagnets Mn2-based full Heusler compounds: Mn_2ZrSi and Mn_2ZrGe, J. Magn. Magn. Mater. 388 (2015) 59–67.
[16] A. Boudali, M. Zemouli, F. Saadaoui, Half-metallicity and structural, electronic and magnetic properties, of ful-Heusler Mn2RhSi and Mn2RhGe: Ab initio predictions, (n.d.).
[17] I. Jum'h, S. Sâad essaoud, H. Baaziz, Z. Charifi, A. Telfah, Electronic and Magnetic Structure and Elastic and Thermal Properties of Mn 2-Based Full Heusler Alloys, J. Supercond. Nov. Magn. 32 (12) (2019) 3915–3926.
[18] L. Fan, F. Chen, C. Li, X. Hou, X. Zhu, J. Luo, Z.-Q. Chen, Promising spintronics: Mn-based Heusler alloys Mn_3Ga, Mn_2YGa (Y= V, Nb, Ta), ScMnVGa, J. Magn. Magn. Mater. 497 (2020), 166060.
[19] D. Bensaid, T. Hellal, M. Ameri, Y. Azzaz, B. Doumi, Y. Al-Douri, B. Abderrahim, F. Benzoudji, First-principle investigation of structural, electronic and magnetic properties in Mn_2RhZ (Z= Si, Ge, and Sn) Heusler alloys, J. Supercond. Nov. Magn. 29 (7) (2016) 1843–1850.
[20] S.A. Sofi, D.C. Gupta, High Pressure-Temperature study on thermodynamics, half-metallicity, transport, elastic and structural properties of Co-based Heusler alloys: A first-principles study, J. Solid State Chem. 284 (2020) 121178, https://doi.org/10.1016/j.jssc.2020.121178.
[21] P. Nehla, V.K. Anand, B. Klemke, B. Lake, R.S. Dhaka, Magnetocaloric properties and critical behavior of $Co_2Cr_{1-x}Mn_xAl$ Heusler alloys, J. Appl. Phys. 126 (2019), 203903.
[22] O. Amrich, M.E. Amine Monir, H. Baltach, S.B. Omran, X.-W. Sun, X. Wang, Y. Al-Douri, A. Bouhemadou, R. Khenata, Half-metallic ferrimagnetic characteristics of Co 2 YZ (Z= P, As, Sb, and Bi) new full-Heusler alloys: a DFT study, J. Supercond. Nov. Magn. 31 (1) (2018) 241–250.
[23] B. Fadila, M. Ameri, D. Bensaid, M. Noureddine, I. Ameri, S. Mesbah, Y. Al-Douri, Structural, magnetic, electronic and mechanical properties of full-Heusler alloys Co2YAl (Y= Fe, Ti): first principles calculations with different exchange-correlation potentials, J. Magn. Magn. Mater. 448 (2018) 208–220.
[24] R. Bala, DFT based study of structural and magnetic properties of full-Heusler compounds, Mater. Today Proc. 3 (6) (2016) 1840–1844.
[25] P. Blaha, K. Schwarz, G. Madsen, D. Kvasnicka, J. Luitz, Wien2k, (2001).
[26] J.P. Perdew, K. Burke, M. Ernzerhof, Generalized Gradient Approximation Made Simple, Phys. Rev. Lett. 77 (18) (1996) 3865–3868.
[27] A.D. Becke, E.R. Johnson, A simple effective potential for exchange, J. Chem. Phys. 124 (2006), 221101.
[28] A. Togo, I. Tanaka, First principles phonon calculations in materials science, Scr. Mater. 108 (2015) 1–5.
[29] G.K. Madsen, D.J. Singh, BoltzTraP. A code for calculating band-structure dependent quantities, Comput. Phys. Commun. 175 (2006) 67–71.
[30] V.L.A. Otero-de-la-Roza, D. Abbasi-Pérez, Gibbs2: A new version of the quasiharmonic model code. II. Models for solid-state thermodynamics, features and implementation, Comput. Phys. Commun. 182 (10) (2011) 2232–2248.
[31] V.L.A. Otero-de-la-Roza, Gibbs2: A new version of the quasi-harmonic model code. I. Robust treatment of the static data, Comput. Phys. Commun. 182 (8) (2011) 1708–1720.
[32] F.D. Murnaghan, The Compressibility of Media under Extreme Pressures, Proc. Natl. Acad. Sci. 30 (9) (1944) 244–247.
[33] S. Ghosh, S. Ghosh, Systematic understanding of half-metallicity of ternary compounds in Heusler and Inverse Heusler structures with 3d and 4d elements, Phys. Scr. 94 (2019), 125001.
[34] L. Pauling, The nature of the interatomic forces in metals, Phys. Rev. 54 (1938) 899.
[35] J.C. Slater, The ferromagnetism of nickel. II. Temperature effects, Phys. Rev. 49 (1936) 931.
[36] M. Born, R. Oppenheimer, Zur quantentheorie der molekeln, Ann. Phys. 389 (20) (1927) 457–484.
[37] W. Voigt, Lehrbuch der Kristallphysik (Teubner, Leipzig, 1928), Google Sch. 962 (1908).
[38] A. Reuss, Calculation of the flow limits of mixed crystals on the basis of the plasticity of monocrystals, Z Angew Math Mech. 9 (1929) 49–58.
[39] R Hill, The elastic behaviour of a crystalline aggregate, Proc. Phys. Soc. Sect. A. 65 (5) (1952) 349–354.
[40] M. Jamal, S. Jalali Asadabadi, Iftikhar Ahmad, H.A. Rahnamaye Aliabad, Elastic constants of cubic crystals, Comput. Mater. Sci. 95 (2014) 592–599.
[41] M. Born, K. Huang, Dynamical theory of crystal lattices, Clarendon press (1954).
[42] S.F. Pugh, XCII. Relations between the elastic moduli and the plastic properties of polycrystalline pure metals, Lond. Edinb. Dublin Philos. Mag. J. Sci. 45 (1954) 823–843.
[43] L. Kleinman, Deformation potentials in silicon. I. Uniaxial strain, Phys. Rev. 128 (1962) 2614.
[44] P. Debye, Einige bemerkungen zur magnetisierung bei tiefer temperatur, Ann. Phys. 386 (25) (1926) 1154–1160.
[45] A. Otero-de-la-Roza, V. Luaña, Gibbs2: A new version of the quasi-harmonic model code. I. Robust treatment of the static data, Comput. Phys. Commun. 182 (2011) 1708–1720.
[46] A. Otero-de-la-Roza, D. Abbasi-Pérez, V. Luaña, Gibbs2: A new version of the quasiharmonic model code. II. Models for solid-state thermodynamics, features and implementation, Comput. Phys. Commun. 182 (2011) 2232–2248.
[47] P.L. Dulong, A.-T. Petit, Recherches sur quelques points importans de la theorie de la Chaleur, 1819.
[48] G.A. Slack, Nonmetallic crystals with high thermal conductivity, J. Phys. Chem. Solids. 34 (2) (1973) 321–335.